Histone phosphorylation by TRPM6's cleaved kinase attenuates adjacent arginine methylation to regulate gene expression

Grigory Krapivinsky[a,b], Luba Krapivinsky[a,b], Nora E. Renthal[c], Ana Santa-Cruz[a,b], Yunona Manasian[a,b], and David E. Clapham[a,b,d,1,2]

[a]Howard Hughes Medical Institute, Boston Children's Hospital, Harvard Medical School, Boston, MA 02115; [b]Department of Cardiology, Harvard Medical School, Boston, MA 02115; [c]Division of Endocrinology, Boston Children's Hospital, Harvard Medical School, Boston, MA 02115; and [d]Department of Neurobiology, Harvard Medical School, Boston, MA 02115

Contributed by David E. Clapham, July 10, 2017 (sent for review May 21, 2017; reviewed by Gail Mandel and Dejian Ren)

TRPM6 and TRPM7 are members of the melastatin-related transient receptor potential (TRPM) subfamily of ion channels. Deletion of either gene in mice is embryonically lethal. TRPM6/7 are the only known examples of single polypeptides containing both an ion channel pore and a serine/threonine kinase (chanzyme). Here we show that the C-terminal kinase domain of TRPM6 is cleaved from the channel domain in a cell type-specific fashion and is active. Cleavage requires that the channel conductance is functional. The cleaved kinase translocates to the nucleus, where it is strictly localized and phosphorylates specific histone serine and threonine (S/T) residues. TRPM6-cleaved kinases (M6CKs) bind subunits of the protein arginine methyltransferase 5 (PRMT5) molecular complex that make important epigenetic modifications by methylating histone arginine residues. Histone phosphorylation by M6CK results in a dramatic decrease in methylation of arginines adjacent to M6CK-phosphorylated amino acids. Knockout of *TRPM6* or inactivation of its kinase results in global changes in histone S/T phosphorylation and changes the transcription of hundreds of genes. We hypothesize that M6CK associates with the PRMT5 molecular complex in the nucleus, directing M6CK to a specific genomic location and providing site-specific histone phosphorylation. M6CK histone phosphorylation, in turn, regulates transcription by attenuating the effect of local arginine methylation.

TRPM6 | TRPM7 | kinase | ion channel | PRMT5

Among the several hundred genes encoding cation channels, the melastatin-related transient receptor potential family members TRPM6 and TRPM7 are unique in also being serine/threonine (S/T) kinases (1). The TRPM6 channel kinase was brought to greater attention when mutations in this chanzyme were found to be the cause of familial hypomagnesemia with secondary hypocalcemia (HSH; see ref. 2 for a recent review). Characterized by severe hypomagnesemia, infants with HSH suffer tetany and refractory seizures shortly after birth, resulting in permanent neurological damage or death if untreated. The mechanisms by which mutations in *TRPM6* lead to HSH are unknown, although several studies stress the importance of TRPM6-mediated Mg^{2+} conductance (3–5). Importantly, global *TRPM6* disruption in mice is embryonic lethal (6, 7). Mice with loss of *TRPM6* at intermediate developmental time points manifest a reduced life span and skeletal deformations, in addition to mild hypomagnesemia (5). These data indicate that, much like *TRPM7* (8), *TRPM6* may be critical for normal, developmental, tissue-specific regulation of gene activity.

Recently, our laboratory uncovered a signaling pathway mediated by TRPM7, a channel sharing 52% homology with TRPM6, whereby the functional S/T kinase at the carboxyl terminus of TRPM7 is proteolytically cleaved from the channel domain, forming cleaved kinase fragments (M7CKs) that translocate to the nucleus (9). There, M7CKs bind components of chromatin-remodeling complexes to ultimately phosphorylate specific S/T residues of histones, regulate selected histone acetylation, and modulate gene transcription.

The present study investigates whether the TRPM6 kinase may play a similar role in cells to direct gene expression. Although TRPM6 is known to undergo autophosphorylation, little else is understood regarding the phosphorylation targets of TRPM6 and the functional role of its kinase (10–12). Furthermore, whether there are links between the conductance of the TRPM6 channel and the activity of its kinase is unknown.

Here we show that the TRPM6 kinase is cleaved from the channel domain in a cell type-specific fashion and that kinase cleavage requires the TRPM6 channel's conductance. TRPM6-cleaved kinases (M6CKs) localize strictly to the nucleus and phosphorylate select S/T residues of histones. M6CKs bind the protein arginine methyltransferase 5 (PRMT5) molecular complex, which has been shown to direct important epigenetic modifications by methylating histone arginines (13). Histone phosphorylation by M6CK results in a dramatic decrease in the methylation of arginine residues adjacent to M6CK-phosphorylated amino acids. Knockout of the *TRPM6* gene results in global changes in histone S/T phosphorylation and in the transcriptional activity of hundreds of genes. We hypothesize that the association of M6CK with the

Significance

Ion channels are proteins that span the cell's membrane and affect the rapid transfer of ions. Kinases are proteins that transfer a phosphate from ATP to specific substrates. In mammals, there are two unusual proteins, melastatin-related transient receptor potential (TRPM)6 and TRPM7, that have both functions. Here we show that TRPM6's kinase and channel domains are functionally connected: The kinase is cleaved from the channel domain, and this cleavage depends on the channel being operational. The freed kinase moves to the nucleus and phosphorylates specific histone residues. This results in a dramatic decrease in methylation of adjacent arginine amino acids shown to be critical epigenetic marks for cell differentiation and embryonic development. TRPM6's kinase-dependent histone posttranslational modifications change the transcription of hundreds of genes.

Author contributions: G.K. and D.E.C. designed research; G.K., L.K., N.E.R., A.S.-C., and Y.M. performed research; G.K., L.K., and Y.M. contributed new reagents/analytic tools; G.K., N.E.R., A.S.-C., and D.E.C. analyzed data; and G.K., N.E.R., and D.E.C. wrote the paper.

Reviewers: G.M., Oregon Health and Science University; and D.R., University of Pennsylvania.

The authors declare no conflict of interest.

[1]Present address: Howard Hughes Medical Institute, Janelia Research Campus, Ashburn, VA 20147.

[2]To whom correspondence should be addressed. Email: claphamd@janelia.hhmi.org.

This article contains supporting information online at www.pnas.org/lookup/suppl/doi:10.1073/pnas.1708427114/-/DCSupplemental.

www.pnas.org/cgi/doi/10.1073/pnas.1708427114

PRMT5 molecular complex in the nucleus directs M6CK to a specific genomic location to provide site-specific histone phosphorylation to attenuate the effect of arginine methylation on transcription.

Results

The C Terminus of TRPM6 Is Proteolytically Cleaved in Vivo, Releasing the Kinase from the Transmembrane Domains. To characterize the endogenous TRPM6 protein and decrease off-target antibody labeling, we first immunoprecipitated the protein from 2 to 3×10^7 cells using a rabbit antibody (made to the C-terminal 14 amino acids of TRPM6; αM6C14), followed by Western blotting (WB) with a mouse antibody recognizing the C-terminal epitope. We tested a number of cell types and found three cell lines where native TRPM6 protein expression was robustly detected (Fig. 1*A*). In addition to a 230-kDa band corresponding to full-length TRPM6, we detected several lower-molecular mass bands (Fig. 1*A*). As with TRPM7 (9), we suggest that the endogenous TRPM6 molecule is proteolytically cleaved, freeing the kinase domain from the channel moiety. All subsequent experiments were performed in HEK 293T (293T) cells.

Lower-molecular mass bands appear to be true fragments of TRPM6, as deletion of the *TRPM6* gene in 293T cells eliminated all protein bands detected by WB (Fig. 1*A*). Stable ectopic expression of C-terminally HA-tagged TRPM6 in 293T cells also produced multiple M6CKs, detected by HA-IP (immunoprecipitation) followed by HA-WB (Fig. 1*B*). We attribute the observation that overexpressed TRPM6 demonstrates more cleaved fragments than endogenous TRPM6 to the fact that the recognition epitope of the mouse monoclonal antibody used for detection of endogenous TRPM6 is located upstream of amino acid ~1400 (e.g., this antibody does not recognize fragments cleaved between amino acid 1400 and the C terminus; Fig. S1). It is also likely that the avidity of the highly selected HA antibody is superior to that of the mouse monoclonal antibody.

To reveal all endogenous TRPM6 kinase-containing fragments, we used CRISPR-Cas9 techniques to incorporate a 2×HA epitope tag sequence into *TRPM6* immediately before the stop codon (293T-$M6_{HA}$). The cleavage pattern of endogenous HA-tagged TRPM6 protein was identical to that of ectopically expressed protein (Fig. 1*B*). This result argues against the possibility that the

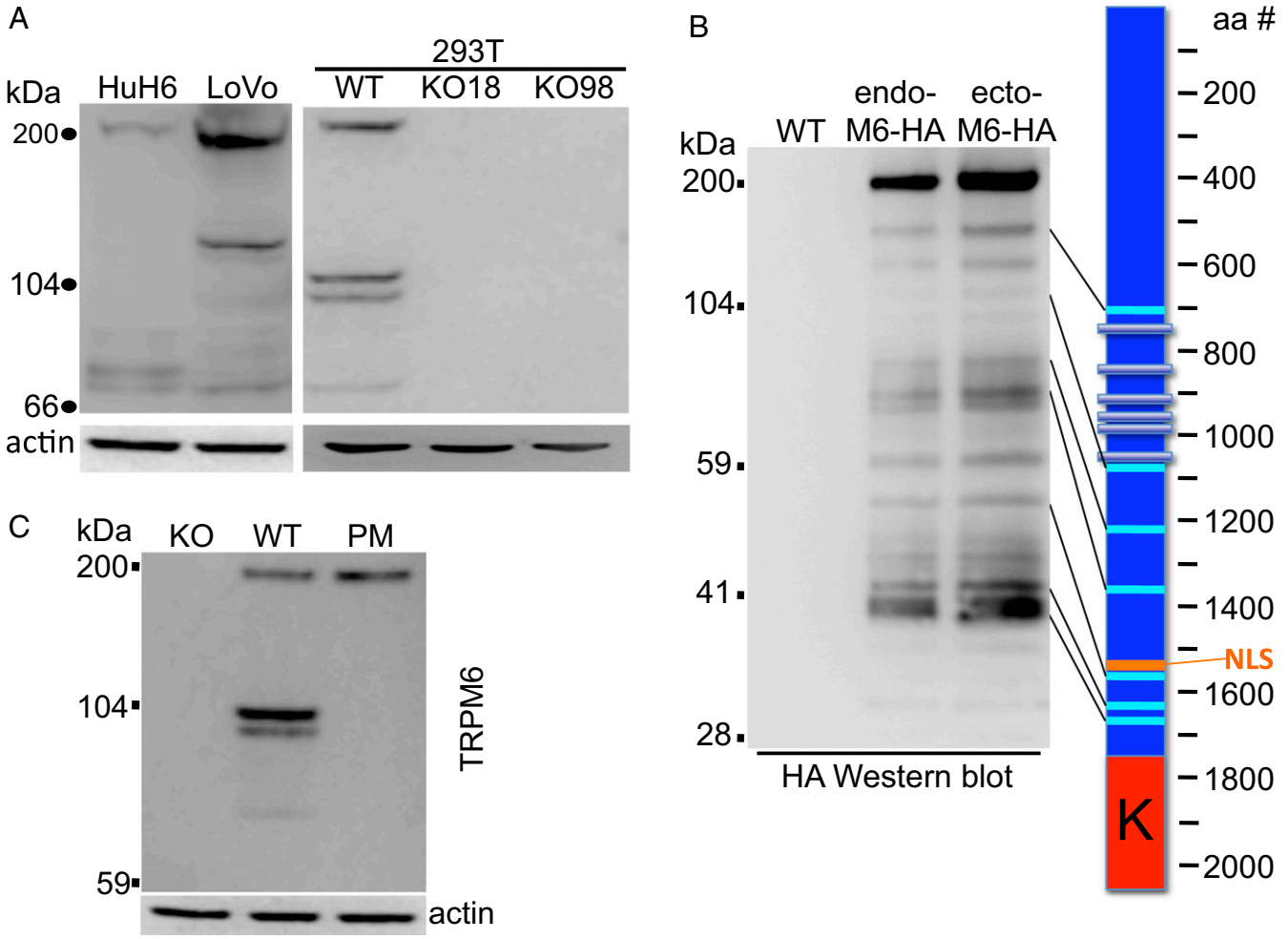

Fig. 1. In vivo TRPM6 cleavage releases its kinase from the channel domain. (*A*) Endogenous TRPM6 extracted from 2.5×10^7 LoVo (human colon), HuH6 (human hepatoblastoma), and 293T (human embryonic kidney) cells, immunoprecipitated from lysates with TRPM6 C-terminal rabbit antibody (αM6C14), and probed on Western blot with mouse TRPM6 antibody. (*A*, *Right*) 293T parental (WT) and *TRPM6*$^{-/-}$ clonal (KO18 and KO98) cells. (*B*) Lysates of WT 293T and 293T cells with endogenous C-terminally 2×HA-tagged TRPM6 (endo-M6-HA) immunoprecipitated with αM6C14 antibody. 293T cells stably expressing ectopic C-terminally HA-tagged TRPM6 (ecto-M6-HA) immunoprecipitated with αHA agarose. All IPs were probed on WB with αHA-peroxidase conjugate. (*B*, *Right*) TRPM6 protein NP_060132.3: the approximate position of the cleavage sites calculated from their electrophoretic mobility relative to standard molecular-mass markers; aa, amino acid; K, kinase domain; NLS, predicted nuclear localization signal. (*C*) The TRPM6 channel conductance is required for the proteolytic release of the kinase domain. Endogenous TRPM6 protein was detected as in *A* in *TRPM6*$^{-/-}$ (KO), parental (WT), and endogenous *TRPM6* pore mutant (PM) 293T cells.

detected TRPM6 fragments are products of alternative splicing. In addition, we conclude that these fragments are not the result of proteolysis during IP, because their relative abundance did not vary with time over 2 to 17 h.

We next sought to investigate whether the channel activity of TRPM6 is required for cleavage of M6CKs from the channel domain. Using CRISPR-Cas9, we introduced a pore mutation in the sixth transmembrane domain of TRPM6 in 293T-$M6_{HA}$ cells (amino acids 1063 to 1065, NLL to FAP), which eliminated the channel's conductance (Fig. S2). We previously demonstrated that an identical TRPM7 pore mutant acted as a dominant negative, preventing ion conduction by the native channel (14). We found that pore mutations in TRPM6 did not effect TRPM6 expression but completely abolished endogenous protein cleavage (Fig. 1*C*). These data support the conclusion that TRPM6's C terminus is proteolytically cleaved in vivo and suggest that conductance of the TRPM6 channel is required for kinase cleavage. Hence, channel activity regulation will be mirrored in kinase release.

Nuclear Localization of M6CKs. The heterologously expressed full-length TRPM6 is localized to intracellular vesicles (Fig. 2*A*) similar to TRPM7-containing vesicles (15) and colocalizes with TRPM7. Unfortunately, very low expression of endogenous TRPM6 hindered our ability to further resolve its cellular location, even with high-avidity HA antibodies. M6CKs cleaved at amino acids 1100, 1225, and 1365 were localized strictly in the nucleus by immunofluorescence (Fig. 2*B*). M6CK cleaved at amino acid 1658 was localized to both the nucleus and cytoplasm. Analysis of the TRPM6 amino acid sequence (nls-mapper.iab.keio.ac.jp/cgi-bin/NLS_Mapper_form.cgi) predicted several putative nuclear localization signals (NLSs) on the C terminus after the sixth transmembrane domain, that may provide the basis for importin-mediated M6CK nuclear localization (see the position for the highest-score NLS in Fig. 1*B*). In interphase cells, nuclear M6CKs display a granular pattern, suggesting M6CK binding to specific chromatin loci (Fig. 2*B*). This interpretation was supported by the observation that M6CK extraction from nuclei required high salt concentrations (0.4 to 0.6 M NaCl),

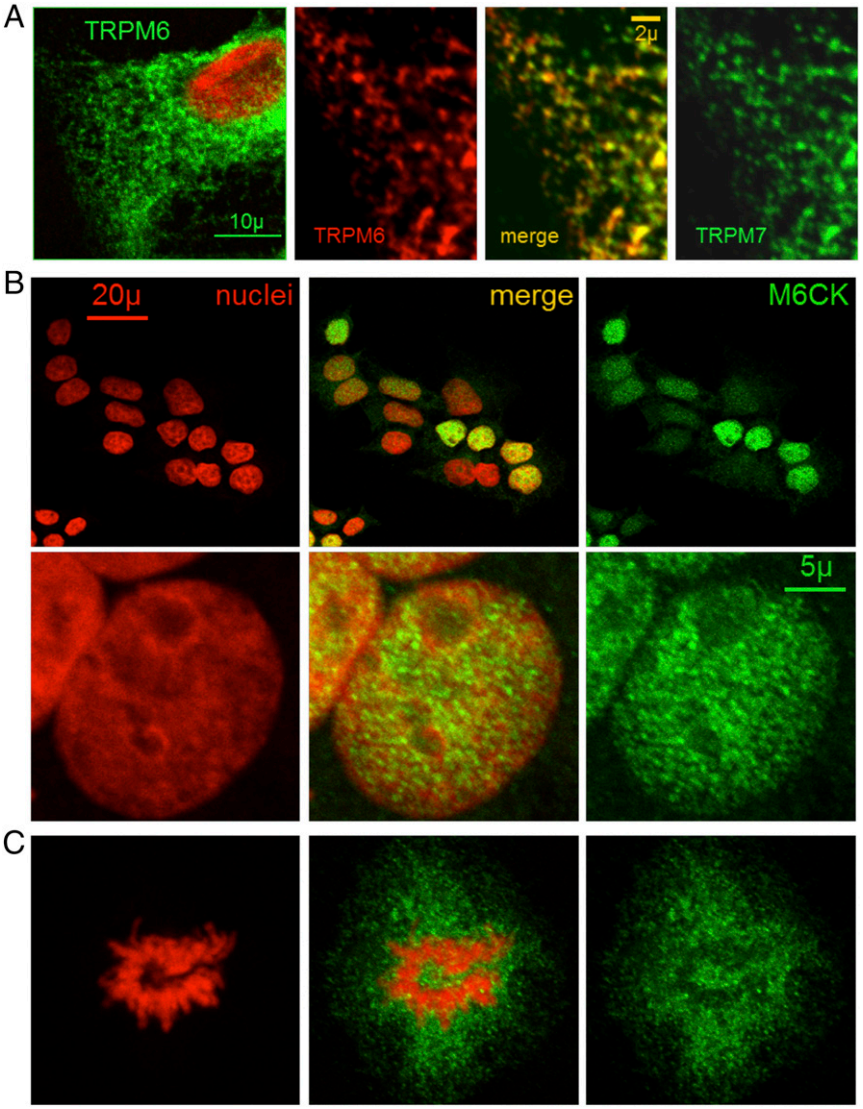

Fig. 2. Nuclear localization of M6CK. (*A*) 293T cells stably expressing FLAG-tagged full-length TRPM6. Fixed cells were labeled with antibody to FLAG and DNA was labeled with DAPI (red, panel 1). Panels 2 to 4 show colocalization of TRPM6 and TRPM7 in 293T cells stably expressing FLAG-tagged full-length TRPM6 and transiently transfected with GFP-tagged TRPM7. (*B*) M6CK-HA (first amino acid is 1365 of full-length TRPM6) stably expressed in 293T cells localized to nuclei in interphase cells. Fixed cells labeled with anti-HA antibody. (*C*) M6CK is excluded from the DNA in mitotic cells (cells and labeling are as in *B*).

similar to conditions for chromatin-bound nuclear proteins. In mitotic cells, M6CK was excluded from chromatin structures (Fig. 2*C*).

M6CKs Tune Gene Transcription. We previously demonstrated that M7CKs translocate to the nucleus to regulate the activity of hundreds of genes (9). The nuclear localization of M6CKs and the structural similarity of M6/M7 channel kinases motivated us to test the effect of TRPM6 on gene activity. We performed microarray analysis for differential gene expression in WT and *TRPM6*$^{-/-}$ 293T cells. Microarray data (Dataset S1) demonstrated that cellular deletion of *TRPM6* is associated with changes in expression of more than 2,000 genes. Functional annotation of differentially expressed genes (16) reveals significant enrichment of genes with nuclear and organelle lumen function (Table S1). To further validate our microarray data, we selected several genes that were highly down-regulated in *TRPM6*$^{-/-}$ cells and performed gene expression analysis with quantitative PCR (qPCR). Comparison of gene expression in WT 293T and 293T-*TRPM6*$^{-/-}$ cells confirmed the microarray data (Fig. 3). To distinguish whether the activity of the TRPM6 channel or its kinase was responsible for modulating gene expression, we generated 293T cells with a point mutation in the phosphotransferase domain (K1804A) of *TRPM6*. As shown in Fig. S2, this mutation eliminated TRPM6 kinase activity but did not change the channel's conductance or endogenous full-length *TRPM6* protein expression. TRPM6 kinase inactivation reproduces *TRPM6*$^{-/-}$-dependent changes in gene activity (Fig. 3). We conclude that TRPM6's kinase activity is responsible for *TRPM6* deletion-dependent alterations in gene expression.

M6CK Binds Components of the PRMT5 Complex. To gain insight into the cellular mechanisms regulated by M6CKs, we studied the TRPM6 interactome, harnessing tandem affinity purification methodology, followed by mass spectrometry identification of proteins copurified with TRPM6 (17). To reveal M6CK interactors, we chose as bait a full-length, C-terminally tagged TRPM6 stably expressed in 293T cells, as this tagged protein has the same cleavage pattern as endogenous TRPM6 (Fig. 1*B*). These experiments showed a substantial proportion of putative TRPM6 interactors to be nuclear proteins (Dataset S2). The most striking finding in purified TRPM6 molecular complexes was the abundance of PRMT5 and accessory subunits of the PRMT5 methylosome molecular complex WDR77 (13) and ICLN (pICln), along with core spliceosomal proteins (Dataset S2).

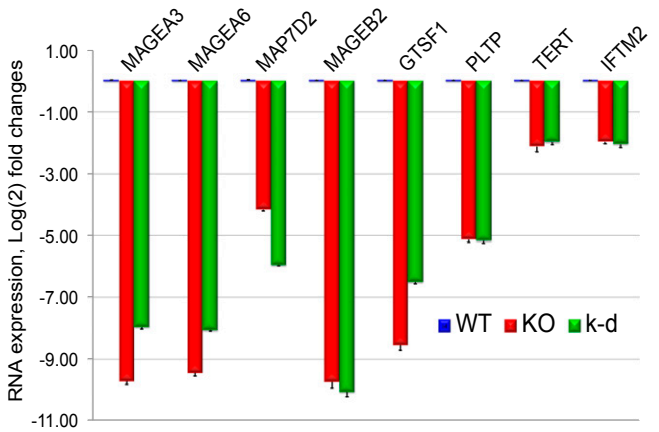

Fig. 3. M6CK tunes gene transcription. Expression of selected genes was quantified by RT-qPCR in 293T wild-type cells (WT), *TRPM6*$^{-/-}$ (KO), and cells with a *TRPM6* genomic single-amino acid mutation (K1804A) inactivating the kinase (kinase-dead; k-d). Data are normalized to expression in WT cells. Error bars represent SD.

To examine whether endogenous TRPM6 complexes with the identified presumed interactors, we immunoprecipitated endogenous TRPM6$_{HA}$ from 293T-M6$_{HA}$ cells with HA antibody and performed WB for endogenous candidate proteins. WT 293T cells were used as controls for the determination of nonspecific binding. Fig. 4*A* demonstrates that PRMT5, WDR77, and ICLN were specifically bound to endogenous TRPM6. To test whether the PRMT5 complex specifically interacts with M6CK, we immunoprecipitated stably, ectopically expressed, FLAG-tagged full-length TRPM6 and M6CK. We found that specific binding of endogenous PRMT5 and subunits of the PRMT5 complex to M6CK cleaved at amino acid 1365 (Fig. 4*B*). M6CK cleaved at amino acid 1658 also binds components of the PRMT5 complex, which suggests that the binding site is located on the C terminus, proximal to the kinase or within the kinase domain. Hence, M6CK binds components of the PRMT5 complex.

M6CK Phosphorylates Specific S/T Residues of Histones and Attenuates Methylation of Adjacent Arginine Residues. We first tested whether bound PRMT5, WDR77, and ICLN were phosphorylated by M6CK in vitro. Epitope-tagged, ectopically coexpressed, and immunoprecipitated M6CK did not phosphorylate coimmunoprecipitated PRMT5, WDR77, or ICLN. We were also unable to detect phosphorylation of purified PRMT5, WDR77, and ICLN proteins with purified M6CK.

PRMT5 is known to symmetrically dimethylate arginine residues in many proteins, including nuclear proteins. This post-translational modification regulates the functional activity of these proteins and is associated with transcriptional regulation (primarily inhibition), apoptosis and cell-cycle progression, DNA repair, and developmental gene regulation (18, 19). Great attention has been paid to PRMT5-mediated methylation of specific arginine residues in histones. These modifications alter chromatin structure by affecting the recruitment of nonhistone proteins that modulate the accessibility of genomic DNA, thus tuning gene expression involved in cell-cycle progression, differentiation, and DNA repair, among other cellular functions (20–23). As we recently demonstrated, the highly homologous M7CK phosphorylates specific histone S/T residues, enhancing neighboring lysine acetylation to alter gene expression (9). Analogously, we hypothesize that binding of M6CK to the PRMT5 complex or its histone-associated subunits may target M6CKs for S/T phosphorylation at specific chromatin locations, adjacent to PRMT5-methylated arginine residues.

Fig. S3 demonstrates that purified M6CK effectively phosphorylates purified histones in vitro. We next compared M6CK-dependent in vivo histone phosphorylation in WT and *TRPM6*-KO 293T cells. Using phospho-specific antibodies, we probed S/T phosphorylation at residues neighboring arginines known to be methylated by PRMT5 (18). In the same chromatin preparations, we tested histone arginine methylation using antibodies specific for selected symmetrically dimethylated arginines (Arg-me2). These experiments demonstrate that knockout of *TRPM6* results in a global decrease in phosphorylation of H2A-S1 and H4-S1 (Fig. 5*A*). To support these findings, we also demonstrated that H2A-S1 and H4-S1 were directly phosphorylated by purified M6CK in preparations of purified H2A and H4 histones (Fig. 5*A*). Coinciding with serine dephosphorylation, deletion of *TRPM6* resulted in a dramatic increase of global symmetric methylation of H2A-R3 and H4-R3, arginines proximal to dephosphorylated serines. For H3 histones, loss of *TRPM6* resulted in dephosphorylation of H3-Thr3 and H3-Thr6, concurrent with a substantial increase in the symmetric methylation of H3-R2 and H3-R8 (Fig. 5*B*). Again, M6CK directly phosphorylated H3-Thr3 and H3-Thr6 (Fig. 5*B*).

We previously demonstrated that TRPM7 kinase phosphorylated H3-S10 and H3-S28 in vivo but did not affect T11 phosphorylation (9). Here we tested phosphorylation of these residues

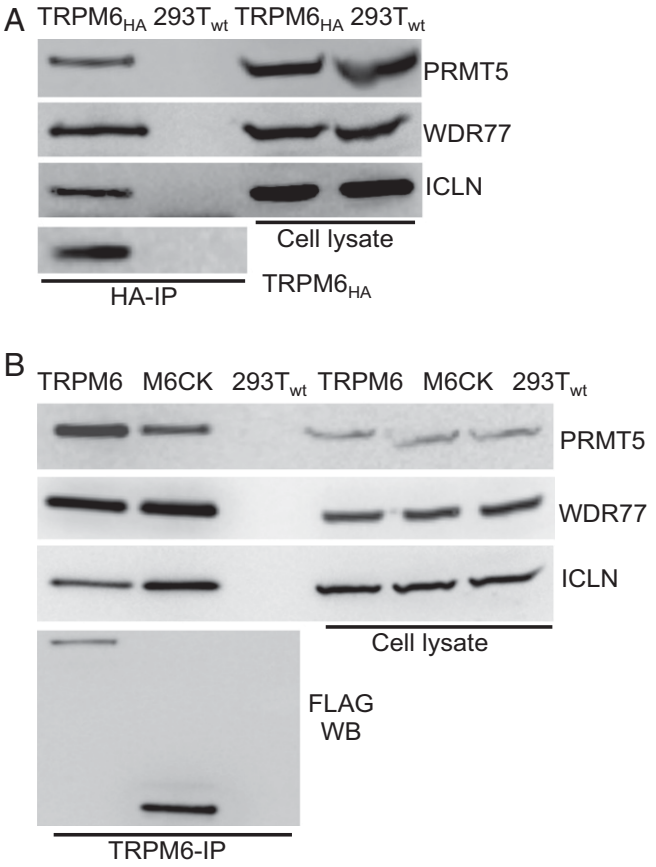

Fig. 4. M6CK binds PRMT5, WDR77, and ICLN subunits of the protein methylase complex. (*A*) Endogenous TRPM6 binds endogenous PRMT5 and associated proteins. Extracts of 293T cells with endogenous HA-tagged TRPM6 ($TRPM6_{HA}$) immunoprecipitated with HA-agarose and probed on WB with antibodies recognizing proteins of interest. Parental 293T cells (WT) served as negative controls. (*B*) Extracts of 293T cells stably expressing FLAG-tagged full-length TRPM6 or M6CK (first amino acid is residue 1365 of full-length TRPM6) immunoprecipitated with FLAG-agarose and probed on Western blot with antibodies recognizing proteins of interest. Parental 293T cells (WT) served as negative controls.

in *TRPM6*-KO cells to investigate whether these two homologous kinases have distinct histone phosphorylation patterns. Unlike TRPM7, we found that loss of TRPM6 resulted in hyperphosphorylation of H3-S10 and H3-T11, implying that TRPM6 does not phosphorylate these serines directly but rather inhibits a separate kinase that modifies these residues (Fig. 5*C*). This conclusion was corroborated by our finding that purified M6CK did not phosphorylate purified H3-S10 and H3-T11 in vitro (Fig. 5*C*). In contrast to TRPM7, phosphorylation of H3-S28 was not affected by deletion of *TRPM6* (Fig. 5*C*), and thus served as an intrinsic control. Antibody recognition of methylated lysine residues may be compromised when an adjacent residue is phosphorylated (24). Similarly, it is possible that a reduction in S/T phosphorylation might mimic adjacent arginine hypermethylation. To test this possibility, we pretreated histone extracts with λ-phosphatase and found that the increased Arg-me2 in $TRPM6^{-/-}$ cells was not affected by histone dephosphorylation.

We also tested histone phosphorylation and methylation in cells where endogenous TRPM6 kinase was inactivated by a selective point mutation in *TRPM6* (*Materials and Methods* and Fig. S2). The kinase-dead mutation attenuated the same histone phosphorylation and enhanced arginine methylation as seen in knockouts of WT *TRPM6* (Fig. 5*D*). We conclude that M6CK itself is responsible for modulation of histone phosphorylation and methylation. This conclusion is supported by the finding that overexpression of active M6CK in *TRPM6*-KO cells reversed TRPM6-dependent histone phosphorylation and methylation to the WT level (Fig. S4). These data indicate that M6CK can directly phosphorylate selected S/T residues in histones and abrogate symmetric methylation of the neighboring arginine residues.

The PRMT5–WDR77–ICLN complex is also critical for core spliceosome biogenesis (25–27). Using co-IP, we found that TRPM6 binds other components of the core spliceosome: SNRPD1, SNRPD2, HNRNPA2B1, SmBB′, and the splicing effector Matrin3 (28) (Dataset S2). These findings suggest that M6CK may participate in RNA splicing regulation, an avenue that will require more detailed future study.

Discussion

We demonstrated that fragments of the TRPM6 C terminus containing the functional protein kinase are cleaved from the channel domain in a cell type-specific fashion. We also demonstrated that mutations ablating TRPM6 channel activity (pore mutants) preclude kinase cleavage, implying that TRPM6 channel activity plays a critical role in the generation of M6CKs. This finding suggests that ions permeating the channel activate or translocate proteases to release the kinase from the channel. We recently demonstrated that the bulk of the homologous TRPM7 chanzyme is localized to unique intracellular vesicles. These vesicles are capable of accumulating Zn^{2+} and releasing it via a TRPM7-dependent mechanism (15). Here we demonstrate that the TRPM6 chanzyme is localized to the membranes of these same vesicles. Because TRPM6, like TRPM7, has been shown to conduct Zn^{2+} (29), we speculate that local [Zn^{2+}] may initiate the kinase domain release mechanism. In the present study, we focused on investigating the targets of released, functional TRPM6 kinase. Future studies will be necessary to further delineate the mechanisms underpinning the regulation of M6CK cleavage, potentially via local [Zn^{2+}]-activated metalloproteases.

We found that M6CKs accumulate in the nucleus, and therefore investigated a nuclear-delimited function for the TRPM6 kinase. As demonstrated by genomic inactivation of TRPM6 kinase activity, M6CKs are involved in transcriptional regulation of more than 2,000 genes in 293T cells. TRPM7 also regulates gene transcription in a set of target genes that are distinct from that of TRPM6 (9). We speculate that TRPM6 and TRPM7 channels destine cells for the expression of divergent transcriptomes via the action of their cleaved kinases. However, because the channel-dependent transcriptomes were studied in cells with different epigenetic landscapes (embryonic stem cells for TRPM7 and embryonic kidney cells for TRPM6) and cells may vary substantially in a variety of factors in the TRPM6/7 pathways, further studies are necessary to understand the initiation and consequences of these transcriptional changes.

Given M6CK's nuclear localization, it was not surprising that our TRPM6 interactome contained an array of nuclear proteins. Among several putative interactors, those most abundantly represented were subunits of the methylosome molecular complex, including PRMT5, WDR77, and ICLN. Endogenous M6CKs also bind these proteins. The principal component of the methylosome is the protein arginine methylase PRMT5, an enzyme that symmetrically dimethylates arginine residues (19). In recent years, the study of histone arginine methylation has attracted great attention. Studies have revealed a critical role for this mechanism in epigenetically controlled cellular processes (30) and the functional significance of specific histone methylation (20–23, 31). WDR77 is required for substrate specificity (32), and may define PRMT5-dependent histone methylation targets (22, 33, 34). ICLN has been shown to modulate PRMT5-dependent histone methylation (33, 35, 36), but its precise function is unknown.

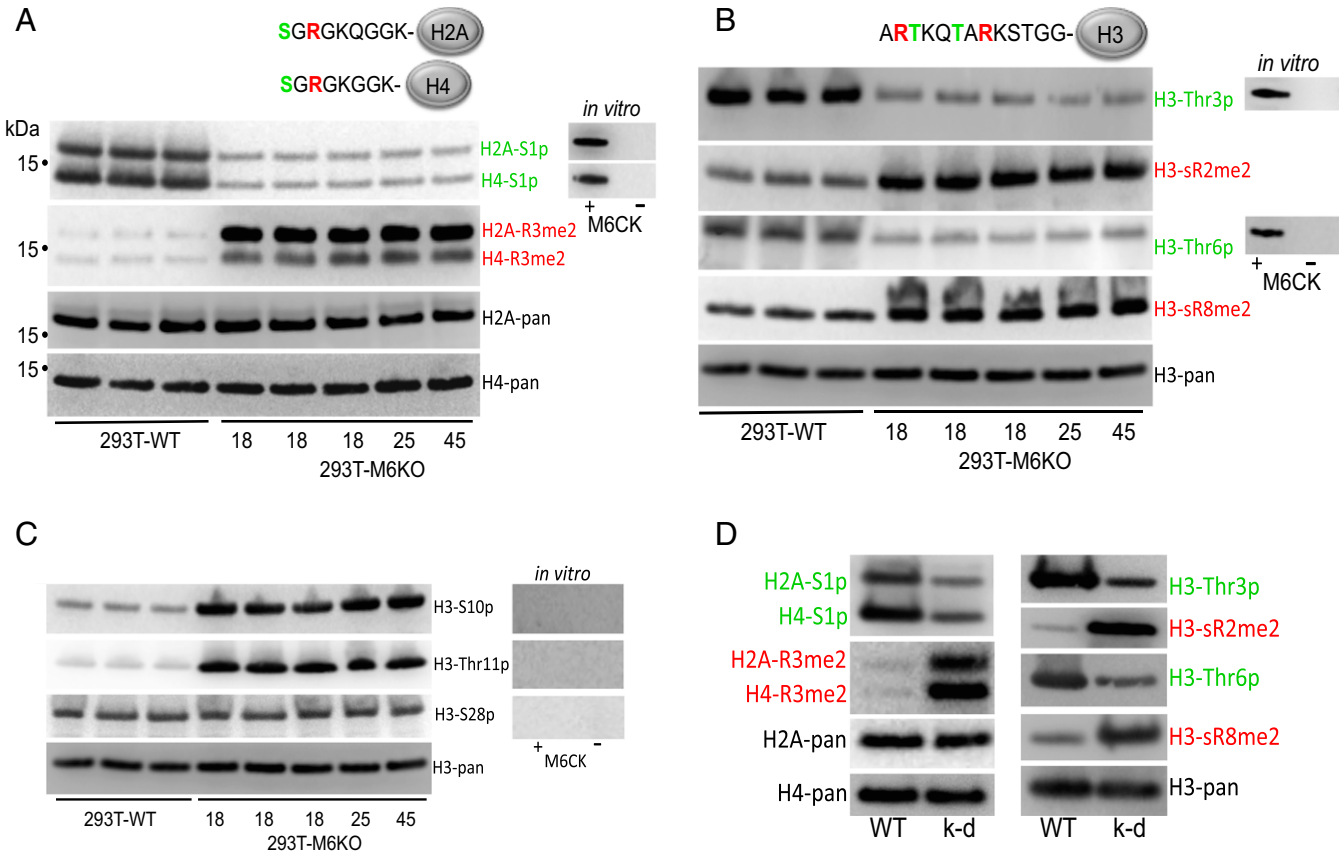

Fig. 5. TRPM6 kinase-dependent global histone phosphorylation and Arg methylation. Western blots of histone extracts with antibody recognizing the indicated posttranslational histone modifications (PTMs). (*A*) Histone H2A-Ser1 and H4-Ser1 phosphorylation (-S1p) and symmetric Arg3 dimethylation (-R3me2). Note that the epitopes in H2A and H4 are nearly identical, enabling the same antibody to be used to recognize modified residues (cartoon; *Top*). Different electrophoretic mobilities of H2A and H4 allow simultaneous measurement of PTM levels in both histones. Histones were extracted from the parental 293T cell (WT; three independent samples) and several clones of 293T-*TRPM6*$^{-/-}$ (KO) cells (clone numbers are shown; three independent samples for clone 18). Pan-antibody recognized all PTMs of the specific histone; there is equal histone content in all samples. (*A*, *Right*) Western blots (same antibodies) of purified recombinant histones phosphorylated in vitro with purified M6CK. (*B*) Histone H3-Thr3 and H3-Thr6 phosphorylation and symmetric Arg2 and Arg8 dimethylation. Labeling as in *A*. (*C*) Deletion of *TRPM6* indirectly enhanced H3-S10 and H3-Thr11 phosphorylation and did not affect H3-S28 phosphorylation in vivo. M6CK did not phosphorylate H3-S10, H3-Thr11, or H3-S28 in vitro (*Right*). Phosphorylation conditions and labeling are as in *A* and *B*. (*D*) Endogenous TRPM6 kinase inactivation (kinase-dead) resulting in the same histone PTM changes as the *TRPM6* knockout.

We found in vivo that M6CK phosphorylates S/T residues of histones adjacent to arginines known to be methylated by PRMT5. Moreover, this phosphorylation substantially attenuated symmetric methylation of these arginines. Thus, our primary hypothesis is that M6CK phosphorylates histone S/T residues near arginines methylated by PRMT5. M6CK's association with PRMT5, WDR77, and ICLN may target M7CK to a specific genomic location to provide site-specific histone phosphorylation that attenuates the effect of the local epigenetic arginine-methylation mark. Our observation of methylation/phosphorylation cross-talk in vivo is directly confirmed by the observation that PRMT5-mediated in vitro methylation of Arg3 in H2A and H4 synthetic peptides was blocked by the phosphorylation of H2A/H4 Ser1 (37). It is also feasible that histone phosphorylation by M6CK serves as an independent epigenetic mark. Further genome-wide studies are required to reveal the correlation between the location of PRMT5-dependent histone methylation and M6CK-dependent histone phosphorylation.

Methylation of histone arginine residues is important in regulation of cell-cycle progression, transcription, DNA repair, and cellular differentiation (19). M6CK's interaction with the PRMT5 molecular complex and inhibition of PRMT5-directed histone methylation by M6CK-directed phosphorylation potentially implicate TRPM6 in the regulation of these functions, opening the door to exciting future studies. In particular, PRMT5-mediated posttranslational histone modification significantly affects gene expression and ultimately induces abnormal cell growth and proliferation (38, 39). Overexpression or dysregulation of PRMT5 has been reported in a number of cancers, including ovarian, breast, lung, lymphoid, lymphoma, melanoma, colon, gastric, prostate, and bladder cancer and germ cell tumors (13, 40, 41). Negative regulation of histone arginine methylation by M6CK raises the possibility that TRPM6 could be used as an endogenous PRMT5 inhibitor to suppress some tumors.

Finally, the present study suggests a much wider role for TRPM6 than magnesium homeostasis, as suggested by the severe phenotype found in *TRPM6*$^{-/-}$ mice. Our data support a mechanism in which histone posttranslational modifications by the channel-dependent TRPM6 kinase contribute to the regulation of transcriptional activity of many other genes affecting development.

Materials and Methods

Cell Culture. LoVo (human colon; ATCC, CCL-229) and 293T (human embryonic kidney; ATCC, CRL-3216) cell lines were maintained according to ATCC guidelines. HuH6 (human hepatoblastoma) cells (CVCL_1296; a generous gift of Arlin Rogers, Tufts University, North Grafton, MA) were cultured in DMEM, 10% FBS. 293T cells stably expressing tagged TRPM6 were obtained by selection with 1 μg/mL puromycin or 200 μg/mL hygromycin and cloned by limiting dilution. After testing the protein expression by WB and immunofluorescence,

5 to 10 independent clones with similar proliferation rates and protein expression were combined and used for experiments.

cDNA Constructs. The human TRPM6 (GenBank, NM_017662) coding sequence was PCR-amplified from a human cDNA library and cloned into pEGFP-C1 to make the GFP-TRPM6 fusion construct. TRPM6 FLAG- and HA-tagged constructs were made in a pPyCAG-IP vector [puromycin resistance; gift of Ian Chambers, University of Edinburgh, Edinburgh (42)]. For stable expression of M6CK in *TRPM6*$^{-/-}$ cells, HA-tagged M6CKs were cloned into pCMV-3Tag-8 (blasticidin resistance; Stratagene). The GST-M6CK-HA construct (encoding TRPM6 amino acids 1658 to 2022) was made in the pGEX-4T1 vector (Amersham). cDNA constructs for mammalian expression of N-terminally HA-tagged PRMT5, WDR77, and CLNSA1 were made in a modified pcDNA6 vector (Invitrogen). Mutations in expression constructs were made by QuikChange Lightning (Agilent).

Biochemical Procedures. For TRPM6 and M6CK immunoprecipitation experiments, proteins were extracted from the cells using NE-PER reagents (Pierce) supplemented with protease and phosphatase inhibitor mixture (Pierce); membrane, cytosolic, and nuclear extracts were combined. For histone extraction, the cell pellet was lysed in NI buffer (20 mM Tris, 50 mM NaCl, 1.5 mM $MgCl_2$, 0.5% Triton X-100) containing protease and phosphatase inhibitor mixture. The insoluble pellet was washed with NI buffer and solubilized in SDS gel-loading buffer with brief sonication. For Arg-me2 WB, histones were dephosphorylated with λ-phosphatase as described (43). GST-M6CK protein was purified from expressing BL21 bacteria using glutathione Sepharose (GE Healthcare) as described (9). Purification of PRMT5, WDR77, and ICLN proteins was as described (44, 45).

Tandem Affinity Purification and Mass Spectrometry. 293T cells stably expressing TRPM6-FLAG-HA were lysed as described above for IP experiments. Tagged TRPM6 was bound to FLAGM2-agarose (Sigma) and extensively washed with BW buffer (10 mM Tris, 150 mM NaCl, 1.5 mM $MgCl_2$, 0.5% Nonidet P-40, protease and phosphatase inhibitor mixture, pH 7.4). Bound proteins were eluted with 1 mg/mL FLAG peptide in BW buffer. FLAG-eluted proteins were bound to HA-agarose (Roche) and washed, and bound proteins were eluted with 1 mg/mL HA-peptide. Purified proteins were pelleted by chloroform/methanol and solubilized in gel-loading SDS buffer. After separation by SDS/PAGE, proteins were stained with Coomassie blue, excised, and in-gel–digested with trypsin. Mass spectrometry analyses used a Thermo Fisher Orbitrap Elite mass spectrometer in the proteomic core facility at the Whitehead Institute for Biomedical Research.

Antibodies. Rabbit polyclonal αM6C14 antibody was derived against a peptide of the C-terminal 14 amino acids (RETGRNSPEDDMQL) of human TRPM6, affinity-purified over immobilized antigen, and used for IP of endogenous TRPM6. Mouse monoclonal TRPM6 antibody (Santa Cruz; sc-365536) was used for WB of the immunoprecipitated TRPM6. Rabbit PRMT5 and WDR77 antibodies were as described (44, 45). Commercially available antibodies were as follows: mouse pICLN (Santa Cruz; sc-271327); mouse HA-HRP and HA affinity matrix (Roche); mouse FLAG-M2 agarose and HRP conjugate (Sigma); H2A (12349), H3 (4499), H3S10p (9701), H3S28p (9713), H3Thr3p (9714), and H3Thr11p (9767) antibodies (Cell Signaling); H2A-symR3Me2 (PTM-673), H3-symR2Me2 (PTM-674), and H4-symR3me2 (PTM-639) (PTM Bio); H2A/H4-S1p (Active Motif; 39115); and H3-Thr6p (GeneTex; GTX60916).

Microarray Expression Profiling. Microarray expression profiling was performed on Human Transcriptome Array 2.0 (Affymetrix) at the Microarray and Sequencing Resource, Boston University Medical School.

qPCR Primers.

GAPDH: forward: 5′-TGTTGCCATCAATGACCCCTT-3′, reverse: 5′-CTCCACGACGTACTCAGCG-3′

MAGEA3: forward: 5′-TGTGATCTTCAGCAAAGCTTCCAG-3′, reverse: 5′-TCCATCAGCTCGATGCCAAAGAC-3′

MAGEA6: forward: 5′-ACCTCGCATTTCCTACCCACTC-3′, reverse: 5′-AGGAGGCAGTGGAAACTAAGGG-3′

MAP7D2: forward: 5′-ACGGAGCCTCCCATGAATAAACG-3′, reverse: 5′-TGCATGTGATGAGCTCGGTCTG-3′

MAGEB2: forward: 5′-AGTCAAGCCATCATGCCTCGTG-3′, reverse: 5′-GCCTCTTCTTCCTCTGCTTCAGTG-3′

GTSF1: forward: 5′-AGACTCTGGCTGAGAGCACTTG-3′, reverse: 5′-TATGTTGCTCGCAGGGCTGTTG-3′

PLTP: forward: 5′-TTGGGAGCATTGTCCTGCTGAG-3′, reverse: 5′-TAGCAGTGACAGAGATGGTGGTG-3′

TERT: forward: 5′-CGACATGGAGAACAAGCTGT-3′, reverse: 5′-AGGTGAGACTGGCTCTGAT-3′

IFTM2: forward: 5′-CCACATTGTGCAAACCTTCTCTCC-3′, reverse: 5′-TGCTCCTCCTTGAGCATCTCGTAG-3′

CRISPR-Cas9–Mediated Genome Editing. CRISPR-Cas9–mediated genome editing in 293T cells was performed using homology-directed repair (46). The optimal CRISPR-Cas9 cleavage site was chosen using DESKGEN software (www.deskgen.com). Synthetic CRISPR-Cas9 RNA (crRNA), synthetic *trans*-activating crRNA (tracrRNA), recombinant purified *Streptococcus pyogenes* Cas9 nuclease (spCas9) protein, and 200-nt synthetic donor single-stranded DNA (ultramer) were purchased from IDT and transfected into cells using CRISPRMAX (Invitrogen) or nucleofection (Lonza) as described (47). Donor DNA contained desirable modifications of the genomic sequence (stop codons, coding nucleotide mutations, or additional coding sequences) or silent mutations to make unique PCR priming sites for genotyping and to introduce unique restriction sites for homo/heterozygosity tests. To increase the homologous recombination rate, cells were synchronized in G2/M phase using 200 ng/mL nocodazole (48) for 16 h before transfection. Transfected cells were kept in media containing HDR enhancer, 10 μM RS-1 (49), for 2 d and then cloned by limiting dilution. Genomic DNA extracts (Epicentre) from clonal cells were genotyped by PCR with one primer unique for the incorporated donor and another for annealing with the genomic sequence outside the donor sequence. Genomic DNA from positively genotyped clones was PCR-amplified with primers annealing 100 to 200 nt outside the donor sequence. Amplified fragments were digested with restriction enzyme to identify clones with donor-specific unique restriction sites integrated into both chromosomes. Genomic DNA fragments of selected clones were PCR-amplified with primers annealing 100 to 200 nt outside the donor sequence, cloned into pJet1.2, and sequenced. Clones with the predicted donor incorporation were used in further experiments.

2×HA-Tag Knockin. Cas9 cleavage site: Chr9[74,724,609], TRPM6 NC_000009.12, exon 39.

Target sequence: 5′-ATATGCAACTATAAAAAGGG-3′.

Donor sequence (contains a ZraI unique site; in bold): 5′-TAGAATCAGCTGAGGAGCCTCCAGCAAGGGAGACGGGTAGAAATTCCCCAGAAGATGATATGCAACTATA**CCCATACGATGTTCCAGATTACGCTGGCAGCTATCCTTATGACGTCCCTGATTATGCGTAG**GGAGGAGCAAGAAGATCCCAGTGCTTGCCCTGCCTGCCAGGAACTCTGTGATAACATAGATTGATCAAC-3′.

Genotyping primers: forward: 5′-CCCTGCTCCCATAAACAGCA-3′, reverse: 5′-GCATAATCAGGGACGTCATAAGG-3′.

Homo/heterozygosity primers: forward: 5′-GAAAGGAGGCTTAATCTAGACATGG-3′, reverse: 5′-CTTTAATGTGCAGGATTCTGCTC-3′.

Pore mutation: nucleotides AAC CTG TTG (3187:3195 of NM_017662 coding) >TTC GCA CCG; amino acids NLL (1063 to 1065 of NP_060132.3)>FAP. Cas9 cleavage site: Chr9[74,782,376], TRPM6 exon 23.

Target sequence: 5′-ACTTGAAGAAAGCAATCAACAGG-3′.

Donor sequence (contains a PvuI unique site; in bold): 5′-GTTTGTTCAAGCCAGCCATCCTGCCCTCCTGGTTCTTTTCTTACTCCATTCTTGCAAGCTGTCTACCTCTTCGTGCAATATATCATCATGGT**ATTCGCACCGATCGCG**TTCTTCAAGTAGGTTATTTCAATTAAATATGATTATTTAAATAAGAAATGTGGGCAGATATGTTGAGTAGATTCACATGTACTTTGAGTATG-3′.

Genotyping primers: forward: 5′-GGTATTCGCACCGATCGCG-3′, reverse: 5′-TCACTGTTTCCCATGCTCCA-3′.

Homo/heterozygosity primers: forward: 5′-ATGGTATTCTGTGCAGTTAATGTG-3′, reverse: 5′-TTATTTCACTGTTTCCCATGCTCC-3′.

Kinase mutation: nucleotides AAG (5410 to 5412 of NM_017662 coding)>GCG; amino acid K1804A. Cas9 cleavage site: Chr9[74,782,376], TRPM6 exon 34.

Target sequence: 5′-TTCTTCCTGAGGTTGTGCGG-3′.

Donor sequence (contains a HindIII unique site; in bold): 5′-TGGATGGGGGCCTCCGTAAAGCTATGAGAGTCGTCAGCACTTGGTCTGAGGATGACATTCTCAAGCCGGGACAAGTTTTCATTGTCG**CAAGCTTCTTGCCAGA**GGTAGTCAGAACATGGCATAAAATCTTCCAGGAGAGCACTGTGCTTCATCTTTGCCTCAGGGTAA-GTCTGAAACTCAGAGACCCATAGCCCAGAGGG-3′.

Genotyping primers: forward: 5′-TCTCCCCTTCCCCACATCTA-3′, reverse: 5′-TACCTCTGGCAAGAAGCTTGC-3′.

Homo/heterozygosity primers: forward: 5′-AGTCCCATTCTCCTCTGGTCA-3′, reverse: 5′-AATAGGCTCCCCTTTGGGTT-3′.

TRPM6 knockout: multiple stop codons inserted after base 96 of the coding sequence. Cas9 cleavage site: Chr9[74,858,673], TRPM6 exon 2.

Target sequence: 5′-GTGAGGATTTTTTGAGCTGG-3′.

Donor sequence (contains a ScaI unique site; in bold): 5′-GTATAAAATAATGACACTTTCTTTTTAGTCCCAGAAATCCTGGATTAAAGGAGTATTTGACAAGAGAGAATGTAGCACAATCATACCCAGC**TGAGCGTAGCTGAGTACTG**AAAATTTTCAATTACCTTCTTCTTTTAAAAGCAACACTACCTGATGGACTATTTATAGAAACTTAGAAATATGACTTGTTTAGAAGTTTT-3′.

Genotyping primers: forward: 5′-GGGGTTTGTTCATGTAGGGCT-3′, reverse: 5′-CAGTACTCAGCTACGCTCAGC-3′.

Homo/heterozygosity primers: forward: 5′-AATGCTTAGCCTGTGTGGGG-3′, reverse: 5′-CCTCCCATCAAGAGGAACAGA-3′.

Alternative TRPM6 Knockout in 293T Cells. Microhomology domain-mediated end joining (50) was used to insert puromycin coding sequences followed by SV40-polyA into the second exon of *TRPM6*.

Cas9 cleavage site: Chr9[74,858,731].

Target sequence 5′-CAAATACTCCTTTAATCCAGG-3′ was cloned into the SpCas9 sgRNA expression plasmid BPK1520 (51). Puromycin-SV40pA donor DNA was amplified from pPur (Clontech) with primers that start with 8-nt sequences flanking the CRISPR-Cas9 cleavage site. 293T cells were cotransfected with sgRNA-BPK1520, Cas9-HF1–expressing plasmid VP12 (52), and donor DNA using Lipofectamine LTX (Invitrogen). Three days after transfection, puromycin-resistant cells were selected with 1 μg/mL puromycin for 10 d. Single clones were expanded and genotyped.

Donor primers: forward: 5′-ATCCTGGAACGCTGACATGACCGAGTACAAGCCCAC-3′, reverse: 5′-TCCTTTAAGATGAGTTTGGACAAACCACAAC-3′.

Genotyping primers: forward: 5′-GCCAAAGTGGGACTTGATGGG-3′, reverse: 5′-CGTGGGCTTGTACTCGGTCAT-3′.

Immunofluorescence. Cells were fixed with 4% paraformaldehyde and permeabilized in 0.1% Triton X-100 at room temperature. Nonspecific binding was blocked with 10% goat serum in PBS, and cells were incubated with primary antibodies for 2 h at room temperature or overnight at 4 °C, followed by detection with fluorophore-conjugated secondary antibodies. Nuclei were stained with DAPI in PBS before mounting the cells on slides using ProLong Gold (Life Technologies). Images were acquired on an Olympus Fluoview 1000 confocal microscope.

Electrophysiological Recordings. *TRPM6*-expressing vectors were transiently transfected into 293T-*TRPM7*$^{-/-}$ cells (15). These cells were used for patch-clamp studies of TRPM6 mutants to eliminate the background endogenous TRPM7 current. The cells were voltage-clamped with an Axopatch 200B amplifier controlled via a Digidata 1440A (Molecular Devices). Pipette resistances were 3 to 5 MΩ. The pipette electrode solution contained 120 mM Cs-$MeSO_3$, 8 mM NaCl, 10 mM 1,2-bis(*o*-aminophenoxy)ethane-*N*,*N*,*N*′,*N*′-tetraacetic acid (BAPTA), 2 mM $CaCl_2$, 2 mM ATP-Na_2, and 10 mM Hepes. The bath solution was a modified Hepes-buffered Tyrode's solution, HBT-B, which contained 140 mM NaCl, 5 mM KCl, 2 mM $CaCl_2$, 10 mM Hepes, and 10 mM glucose (pH 7.4). Cells were held at 0 mV, and 200-ms ramps from −100 mV to +100 mV were applied every 2 s. Currents were digitized at 10 kHz and low pass-filtered at 2 kHz.

ACKNOWLEDGMENTS. We thank Svetlana Gapon for help with cell cultures.

1. Runnels LW (2011) TRPM6 and TRPM7: A Mul-TRP-PLIK-cation of channel functions. *Curr Pharm Biotechnol* 12:42–53.
2. Astor MC, et al. (2015) Hypomagnesemia and functional hypoparathyroidism due to novel mutations in the Mg-channel TRPM6. *Endocr Connect* 4:215–222.
3. Komiya Y, Runnels LW (2015) TRPM channels and magnesium in early embryonic development. *Int J Dev Biol* 59:281–288.
4. Blanchard MG, et al. (2016) Regulation of Mg^{2+} reabsorption and transient receptor potential melastatin type 6 activity by cAMP signaling. *J Am Soc Nephrol* 27:804–813.
5. Chubanov V, et al. (2016) Epithelial magnesium transport by TRPM6 is essential for prenatal development and adult survival. *eLife* 5:e20914.
6. Walder RY, et al. (2009) Mice defective in Trpm6 show embryonic mortality and neural tube defects. *Hum Mol Genet* 18:4367–4375.
7. Woudenberg-Vrenken TE, Sukinta A, van der Kemp AW, Bindels RJ, Hoenderop JG (2011) Transient receptor potential melastatin 6 knockout mice are lethal whereas heterozygous deletion results in mild hypomagnesemia. *Nephron Physiol* 117:11–19.
8. Jin J, et al. (2008) Deletion of Trpm7 disrupts embryonic development and thymopoiesis without altering Mg^{2+} homeostasis. *Science* 322:756–760.
9. Krapivinsky G, Krapivinsky L, Manasian Y, Clapham DE (2014) The TRPM7 chanzyme is cleaved to release a chromatin-modifying kinase. *Cell* 157:1061–1072.
10. Clark K, et al. (2008) Massive autophosphorylation of the Ser/Thr-rich domain controls protein kinase activity of TRPM6 and TRPM7. *PLoS One* 3:e1876.
11. Thébault S, et al. (2008) Role of the alpha-kinase domain in transient receptor potential melastatin 6 channel and regulation by intracellular ATP. *J Biol Chem* 283: 19999–20007.
12. Cai N, Bai Z, Nanda V, Runnels LW (2017) Mass spectrometric analysis of TRPM6 and TRPM7 phosphorylation reveals regulatory mechanisms of the channel-kinases. *Sci Rep* 7:42739.
13. Stopa N, Krebs JE, Shechter D (2015) The PRMT5 arginine methyltransferase: Many roles in development, cancer and beyond. *Cell Mol Life Sci* 72:2041–2059.
14. Krapivinsky G, Mochida S, Krapivinsky L, Cibulsky SM, Clapham DE (2006) The TRPM7 ion channel functions in cholinergic synaptic vesicles and affects transmitter release. *Neuron* 52:485–496.
15. Abiria SA, et al. (2017) TRPM7 senses oxidative stress to release Zn^{2+} from unique intracellular vesicles. *Proc Natl Acad Sci USA* 30:E6079–E6088.
16. Huang W, Sherman BT, Lempicki RA (2009) Systematic and integrative analysis of large gene lists using DAVID bioinformatics resources. *Nat Protoc* 4:44–57.
17. Starokadomskyy P, Burstein E (2014) Bimolecular affinity purification: A variation of TAP with multiple applications. *Methods Mol Biol* 1177:193–209.
18. Gayatri S, Bedford MT (2014) Readers of histone methylarginine marks. *Biochim Biophys Acta* 1839:702–710.
19. Blanc RS, Richard S (2017) Arginine methylation: The coming of age. *Mol Cell* 65:8–24.
20. Chittka A, Nitarska J, Grazini U, Richardson WD (2012) Transcription factor positive regulatory domain 4 (PRDM4) recruits protein arginine methyltransferase 5 (PRMT5) to mediate histone arginine methylation and control neural stem cell proliferation and differentiation. *J Biol Chem* 287:42995–43006.
21. Tsai WW, et al. (2013) PRMT5 modulates the metabolic response to fasting signals. *Proc Natl Acad Sci USA* 110:8870–8875.
22. Saha K, Adhikary G, Eckert RL (2016) MEP50/PRMT5 reduces gene expression by histone arginine methylation and this is reversed by PKCδ/p38δ signaling. *J Invest Dermatol* 136:214–224.
23. Chen H, Lorton B, Gupta V, Shechter D (2017) A TGFβ-PRMT5-MEP50 axis regulates cancer cell invasion through histone H3 and H4 arginine methylation coupled transcriptional activation and repression. *Oncogene* 36:373–386.
24. Duan Q, Chen H, Costa M, Dai W (2008) Phosphorylation of H3S10 blocks the access of H3K9 by specific antibodies and histone methyltransferase. Implication in regulating chromatin dynamics and epigenetic inheritance during mitosis. *J Biol Chem* 283: 33585–33590.
25. Meister G, et al. (2001) Methylation of Sm proteins by a complex containing PRMT5 and the putative U snRNP assembly factor pICln. *Curr Biol* 11:1990–1994.
26. Brahms H, Meheus L, de Brabandere V, Fischer U, Lührmann R (2001) Symmetrical dimethylation of arginine residues in spliceosomal Sm protein B/B′ and the Sm-like protein LSm4, and their interaction with the SMN protein. *RNA* 7:1531–1542.
27. Gonsalvez GB, et al. (2007) Two distinct arginine methyltransferases are required for biogenesis of Sm-class ribonucleoproteins. *J Cell Biol* 178:733–740.
28. Coelho MB, et al. (2015) Nuclear matrix protein Matrin3 regulates alternative splicing and forms overlapping regulatory networks with PTB. *EMBO J* 34:653–668.
29. Li M, Jiang J, Yue L (2006) Functional characterization of homo- and heteromeric channel kinases TRPM6 and TRPM7. *J Gen Physiol* 127:525–537.
30. Fuhrmann J, Clancy KW, Thompson PR (2015) Chemical biology of protein arginine modifications in epigenetic regulation. *Chem Rev* 115:5413–5461.
31. Kim S, et al. (2014) PRMT5 protects genomic integrity during global DNA demethylation in primordial germ cells and preimplantation embryos. *Mol Cell* 56:564–579.
32. Antonysamy S, et al. (2012) Crystal structure of the human PRMT5:MEP50 complex. *Proc Natl Acad Sci USA* 109:17960–17965.
33. Aggarwal P, et al. (2010) Nuclear cyclin D1/CDK4 kinase regulates CUL4 expression and triggers neoplastic growth via activation of the PRMT5 methyltransferase. *Cancer Cell* 18:329–340.
34. Burgos ES, et al. (2015) Histone H2A and H4 N-terminal tails are positioned by the MEP50 WD repeat protein for efficient methylation by the PRMT5 arginine methyltransferase. *J Biol Chem* 290:9674–9689.
35. Gu Z, et al. (2012) Protein arginine methyltransferase 5 functions in opposite ways in the cytoplasm and nucleus of prostate cancer cells. *PLoS One* 7:e44033.
36. Lammirato A, et al. (2016) TIS7 induces transcriptional cascade of methylosome components required for muscle differentiation. *BMC Biol* 14:95.
37. Ho MC, et al. (2013) Structure of the arginine methyltransferase PRMT5-MEP50 reveals a mechanism for substrate specificity. *PLoS One* 8:e57008.
38. Scoumanne A, Zhang J, Chen X (2009) PRMT5 is required for cell-cycle progression and p53 tumor suppressor function. *Nucleic Acids Res* 37:4965–4976.
39. Tarighat SS, et al. (2016) The dual epigenetic role of PRMT5 in acute myeloid leukemia: Gene activation and repression via histone arginine methylation. *Leukemia* 30: 789–799.
40. Li Y, et al. (2015) PRMT5 is required for lymphomagenesis triggered by multiple oncogenic drivers. *Cancer Discov* 5:288–303.
41. Deng X, et al. (2017) Protein arginine methyltransferase 5 functions as an epigenetic activator of the androgen receptor to promote prostate cancer cell growth. *Oncogene* 36:1223–1231.
42. Chambers I, et al. (2003) Functional expression cloning of Nanog, a pluripotency sustaining factor in embryonic stem cells. *Cell* 113:643–655.
43. Lau PN, Cheung P (2011) Histone code pathway involving H3 S28 phosphorylation and K27 acetylation activates transcription and antagonizes polycomb silencing. *Proc Natl Acad Sci USA* 108:2801–2806.

44. Pu WT, Krapivinsky GB, Krapivinsky L, Clapham DE (1999) pICln inhibits snRNP biogenesis by binding core spliceosomal proteins. *Mol Cell Biol* 19:4113–4120.
45. Krapivinsky G, Pu W, Wickman K, Krapivinsky L, Clapham DE (1998) pICln binds to a mammalian homolog of a yeast protein involved in regulation of cell morphology. *J Biol Chem* 273:10811–10814.
46. Hsu PD, Lander ES, Zhang F (2014) Development and applications of CRISPR-Cas9 for genome engineering. *Cell* 157:1262–1278.
47. Leonetti MD, Sekine S, Kamiyama D, Weissman JS, Huang B (2016) A scalable strategy for high-throughput GFP tagging of endogenous human proteins. *Proc Natl Acad Sci USA* 113:E3501–E3508.
48. Lin S, Staahl BT, Alla RK, Doudna JA (2014) Enhanced homology-directed human genome engineering by controlled timing of CRISPR/Cas9 delivery. *eLife* 3:e04766.
49. Song J, et al. (2016) RS-1 enhances CRISPR/Cas9- and TALEN-mediated knock-in efficiency. *Nat Commun* 7:10548.
50. Nakade S, et al. (2014) Microhomology-mediated end-joining-dependent integration of donor DNA in cells and animals using TALENs and CRISPR/Cas9. *Nat Commun* 5:5560.
51. Kleinstiver BP, et al. (2015) Engineered CRISPR-Cas9 nucleases with altered PAM specificities. *Nature* 523:481–485.
52. Kleinstiver BP, et al. (2016) High-fidelity CRISPR-Cas9 nucleases with no detectable genome-wide off-target effects. *Nature* 529:490–495.